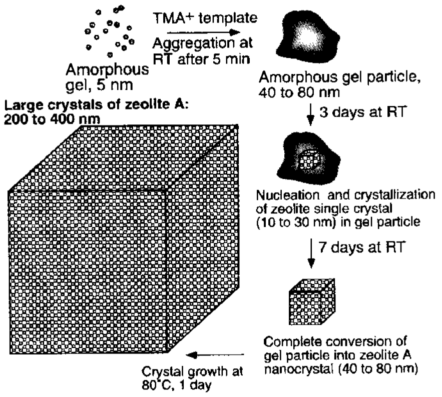

**Fig. 6.** A schematic representation of the proposed zeolite growth mechanism.

that quickly agglomerated after the addition of the organic template to give 40- to 80-nm amorphous aggregates. Zeolite A was nucleated in these aggregates within 3 days at RT. In the system under study, we observed only one single zeolite crystal per amorphous gel particle; thus, aggregation of several nuclei is clearly not needed to achieve crystallization. We propose that high supersaturation within the gel particles, possibly coupled with preorganization at the interface of the amorphous network with occluded solution, is the driving force for nucleation [see also (*14*)]. The amorphous gel-zeolite particles maintained their average size over the course of the complete conversion into (more dense) zeolite A, suggesting that mass transfer from solution supplies some of the precursor material. Solution mass transfer must be the dominant mechanism for the substantial crystal growth in the same zeolite A suspension at elevated temperature (no amorphous precursor material was present), so that solution-mediated transport at RT should also be feasible.

### References and Notes

1. D. W. Breck, *Zeolite Molecular Sieves* (Wiley, London, 1974).
2. M. E. Davis and R. F. Lobo, *Chem. Mater.* **4**, 756 (1992).
3. H. Kessler, in *Solid-State Supramolecular Chemistry: Two- and Three-Dimensional Inorganic Networks*, vol. 7 of *Comprehensive Supramolecular Chemistry*, G. Alberti and T. Bein, Eds. (Elsevier, Tarrytown, NY, 1996), pp. 425–464.
4. S. L. Burkett and M. E. Davis, *ibid.*, pp. 465–483.
5. W. M. Meier, D. H. Olson, Ch. Baerlocher, *Atlas of Zeolite Structure Types* (Elsevier, London, 1996).
6. S. Feng and T. Bein, *Nature* **368**, 834 (1994); *Science* **265**, 1839 (1994); Y. Yan and T. Bein, *J. Am. Chem. Soc.* **117**, 9990 (1995); S. Mintova *et al.*, *Adv. Mater.* **9**, 585 (1997); G. A. Ozin, *ibid.* **4**, 612 (1992); P. Behrens and G. A. Stucky, in *Solid-State Supramolecular Chemistry: Two- and Three-Dimensional Inorganic Networks*, vol. 7 of *Comprehensive Supramolecular Chemistry*, G. Alberti and T. Bein, Eds. (Elsevier, Tarrytown, NY, 1996), pp. 721–772; T. Bein, *Chem. Mater.* **8**, 1636 (1996).
7. T. A. M. Twomey, M. Mackay, H. P. C. E. Kuipers, R. W. Thompson, *Zeolites* **14**, 162 (1994).
8. M. Tsapatsis, M. Lovallo, M. E. Davis, *Micropor. Mater.* **5**, 381 (1996).
9. A. E. Persson, B. J. Schoeman, J. Sterte, J.-E. Otterstedt, *Zeolites* **14**, 557 (1994); B. J. Schoeman, *ibid.* **18**, 97 (1997); *Micropor. Mesopor. Mater.* **22**, 9 (1998); B. J. Schoeman, J. Sterte, J.-E. Otterstedt, *Zeolites* **14**, 110, (1994); J. Dougherty, L. E. Iton, J. W. White, *ibid.* **15**, 640 (1995).
10. G. Zhu *et al.*, *Chem. Mater.* **10**, 1483 (1998).
11. R. Ravishankar *et al.*, *J. Phys. Chem. B.* **102**, 2633 (1998).
12. L. Gora, K. Streletzky, R. W. Thompson, G. D. J. Phillies, *Zeolites* **18**, 119 (1997); L. Gora and R. W. Thompson, *ibid.*, p. 132.
13. C. S. Cundy, B. M. Lowe, D. M. Sinclair, *J. Cryst. Growth* **100**, 189 (1990); C. S. Cundy, M. S. Henty, R. J. Plaisted, *Zeolites* **15**, 342 (1995).
14. S. L. Burkett and M. E. Davis, *J. Phys. Chem.* **98**, 4647 (1994).
15. O. Regev, Y. Cohen, E. Kehat, Y. Talmon, *Zeolites* **14**, 314 (1994).
16. R. W. Corkery and B. W. Ninham, *ibid.* **18**, 379 (1997).
17. W. H. Dokter, H. F. van Garderen, T. P. M. Beelen, R. A. van Santen, W. Bras, *Angew. Chem. Int. Ed. Engl.* **34**, 73 (1995).
18. Very few zeolite syntheses have been reported at low temperature [including (TPA)-silicalite-1, which can be obtained within 18 to 24 months below 35°C (*16*); several beryllophosphates, zincophosphates, and arsenates synthesized at 4° to 100°C (*19*); and zeolite A, which can be obtained from a RT gel after 30 days (*20*)].
19. T. E. Gier and G. Stucky, *Nature* **349**, 508 (1991).
20. L. B. Sand, A. Sacco Jr., R. W. Thompson, A. G. Dixon, *Zeolites* **7**, 387 (1987).
21. For the synthesis of zeolite A, clear aluminosilicate solutions with composition (0.3 to 0.45)$Na_2O$:(4.5 to 12)$SiO_2$:(0.6 to 2)$Al_2O_3$:(9 to 14)$(TMA)_2O$:(400 to 800)$H_2O$ were prepared and mixed at RT on an orbital shaker (175 rpm) for 1 to 10 days. The composition studied most extensively was $0.3Na_2O$:$11.25SiO_2$:$1.8Al_2O_3$:$13.4(TMA)_2O$:$700H_2O$. These systems were prepared with a 30% silica sol (containing NaOH to pH = 10) (Aldrich), aluminium isopropoxide $[Al(OiPr)_3]$ (Aldrich), 97% $TMAOH \cdot 5H_2O$ (Aldrich), NaOH (Mallinckrodt, Chesterfield, MO), and filtered doubly distilled $H_2O$. The gels were prepared from two solutions: Solution I was composed of 2.25 g of 30% silica sol (pH = 10) and 2.0 g of $H_2O$, and solution II was composed of 0.75 g of $Al(OiPr)_3$, 5.00 g of $TMAOH \cdot 5H_2O$, 0.6 g of 1 M NaOH, and 7.0 g of $H_2O$. To start the zeolite synthesis, we mixed the two precursor solutions under stirring. The solid phase contained in the colloidal suspensions (gel or zeolite particles) was recovered by repeated (three times) cycles of ultracentrifugation at 20,000 rpm for 1 hour, decanting, and ultrasonic redispersion in pure water. The growth of zeolite A was also performed at an elevated temperature (80°C for 1 to 2 days), starting with the colloidal suspension that had reacted for 10 days on the shaker at RT.
22. The authors gratefully acknowledge funding from the U.S. National Research Council (Twinning Program) (T.B. and S.M.) and NSF (T.B.). This work was supported by a NIH biology grant to T. S. Baker (GM 33050), a NSF shared equipment grant (to T.S.B., BIR 9112921), and a grant from the Lucille P. Markey charitable trust to the Purdue Structural Biology Center.

14 October 1998; accepted 11 January 1999

---

# Giant Wormlike Rubber Micelles

**You-Yeon Won, H. Ted Davis, Frank S. Bates***

**A low molecular weight poly(ethyleneoxide)-poly(butadiene) (PEO-PB) diblock copolymer containing 50 weight percent PEO forms gigantic wormlike micelles at low concentrations (<5 percent by weight) in water. Subsequent generation of free radicals with a conventional water-based redox reaction leads to chemical cross-linking of the PB cores without disruption of the cylindrical morphology, as evidenced by cryotransmission electron microscopy and small-angle neutron scattering experiments. These wormlike rubber micelles exhibit unusual viscoelastic properties in water.**

Self-assembly of amphiphilic molecules provides a fundamental mechanism for building complex soft materials. Familiar examples include lipid bilayers, the basic element of cell membranes, soap solutions composed of oil containing micellar globules in an aqueous medium, and pressure-sensitive adhesives formulated with ordered block copolymers. By tailoring the molecular architecture and distribution of chemical functionality, discrete supramolecular objects can be created with prescribed shape, size, and state of order. The physical consequences of minor variations in molecular structure can be dramatic, particularly in the dilute limit where small amounts of amphiphile are added to a solvent, often water. This report describes a new type of self-assembled object—giant wormlike micelles that can be chemically cross-linked after dispersion in water. These fixed micelles are actually individual macromolecules with molar masses that are more than three orders of magnitude greater than those typical of large conventional synthetic polymers, $\sim 10^5$ to $10^6$ g/mol. They have a profound effect on the properties of water at small concentrations and can be directly imaged in vitrified aqueous solution by electron microscopy.

During the past few years we have been experimenting with macromolecular surfactants comprised of poly(ethyleneoxide) (PEO) and various hydrocarbon polymers such as poly(butadiene) (PB) and the saturated analog poly(ethylethylene) (PEE) (*1*, *2*). Our PEO-PB (I) and PEO-PEE (II) diblock copolyers,

---

Department of Chemical Engineering and Materials Science, University of Minnesota, Minneapolis, MN 55455, USA.

*To whom correspondence should be addressed.

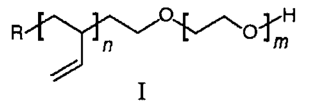

I

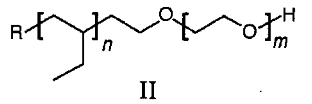

II

are chemically similar to conventional nonionic surfactants often referred to as $C_iE_j$ [for $C_iH_{2i+1}(OCH_2CH_2)_jOH$ where $4 \leq i \leq 22$ and $3 \leq j \leq 12$] except that they are 10 or more times greater in molecular weight. The greater size leads to significantly stronger amphiphilicity and ordered morphologies in water over a wider range of compositions and temperatures (*2*). Here we focus on the water-rich region of the phase diagram. We used nine different PEO-based block copolymers (types I and II) with molar masses ranging from 2.9 to 13.1 kg/mol to verify the sequence of microdomain shape transitions from membrane-like bilayers to cylinders to spheres with increasing PEO composition. Wormlike micelles were observed in the dilute limit over a relatively wide range of PEO weight fractions, $0.47 \leq w_{PEO} \leq 0.59$. This report deals with one of these compounds, **OB3**, a PEO-PB diblock (I) containing 50% by weight PEO, a number average molar mass $\overline{M_N} = 4.9$ kg/mol (that is, $\langle m \rangle = 55$, $\langle n \rangle = 45$), and a polydispersity index of 1.15. It was prepared as described in a published two-step anionic polymerization procedure (*3*).

The phase behavior of aqueous solutions of **OB3** containing up to 17 weight % block copolymer between 25° and 75°C is shown in Fig. 1. At all conditions, the basic morphological unit is cylindrical, with a PB core surrounded by a solvated PEO corona. At block copolymer concentrations $>10\%$, these cylinders are organized on a regular hexagonal lattice, as evidenced by x-ray scattering peaks at the expected sequence of scattering angles. Between 5 and 10% block copolymer in water, the cylindrical domains form a one-dimensional nematic phase. Evidence of the transition from nematic to hexagonal order was obtained from small-angle x-ray and neutron scattering (SAXS and SANS) experiments. At concentrations $<5\%$ block copolymer, these mixtures transform to an isotropic solution containing nonlinear cylindrical structures, often referred to as wormlike micelles. The isotropic-nematic transition was identified through optical birefringence measurements and SANS experiments. Nematic order creates significant birefringence and results in a permanent state of cylinder orientation after being subjected to flow that produces anisotropic SANS patterns. These distinct characteristics are absent in the isotropic phase.

Wormlike micelles were directly imaged in dilute solution by cryo-transmission electron microscopy (CTEM) (*4*, *5*). Thin ($\sim$10 to 300 nm) films of aqueous solution were suspended across holes in a perforated polymer-carbon film–coated TEM copper grid and then vitrified by rapid cooling with liquid ethane ($\sim$90 K). Digital images were obtained by using a JEOL 1210 with a nominal underfocus of $\sim$25 μm to enhance the phase contrast. A representative CTEM micrograph taken from a 1% solution of **OB3** in water is shown in Fig. 2A. Long ($>$1 μm) cylindrical micelles are evident in this image, which reveals dark PB cores dispersed in a light aqueous matrix (*6*).

We selected PB as the micelle core material because the double bonds present on each repeat unit (see I) are readily coupled through standard cross-linking reactions. A water-soluble redox combination of potassium persulfate ($K_2S_2O_8$) and sodium metabisulfite ($Na_2S_2O_5$)–ferrous sulfate ($FeSO_4 \cdot 7H_2O$) was chosen for the initiation of cross-linking. This type of free-radical initiator, used extensively in emulsion polymerizations (*7*), is ideally suited for generating a specified number of radicals in the aqueous phase that are subsequently captured by the nanoscopic micelles. In this work, we produced a relatively high concentration of radicals, one for every two PB double bonds, thereby ensuring a high degree of cross-linking. Although we have not determined the exact cross-link density for the chemically fixed micelles, experiments indicate that every block copolymer has been covalently bonded together within individual giant wormlike molecules. For example, extraction with chloroform, which efficiently removes unreacted block copolymers from aqueous solution, fails to recover any detectable **OB3** from the cross-linked system.

A representative CTEM image of a 0.05% cross-linked solution is shown in Fig. 2B. Within the resolution of this technique the cross-linked and pristine wormlike micelles appear to be indistinguishable (*8*). A more quantitative comparison of the core diameters before and after cross-linking was obtained by SANS. Figure 3A shows SANS results taken from unreacted and cross-

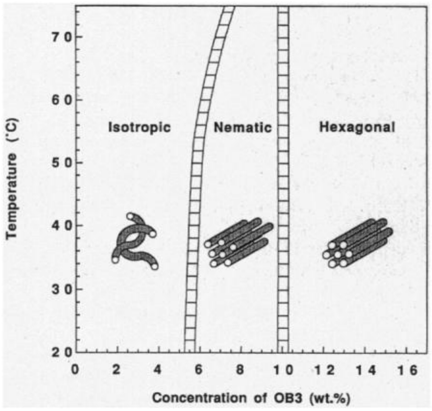

**Fig. 1.** Aqueous phase behavior of sample **OB3**, a diblock copolymer of PEO and PB containing 50 weight % PEO. Phase boundaries were determined by SANS, SAXS, and birefringence measurements. Actual width of the two-phase windows was not resolved.

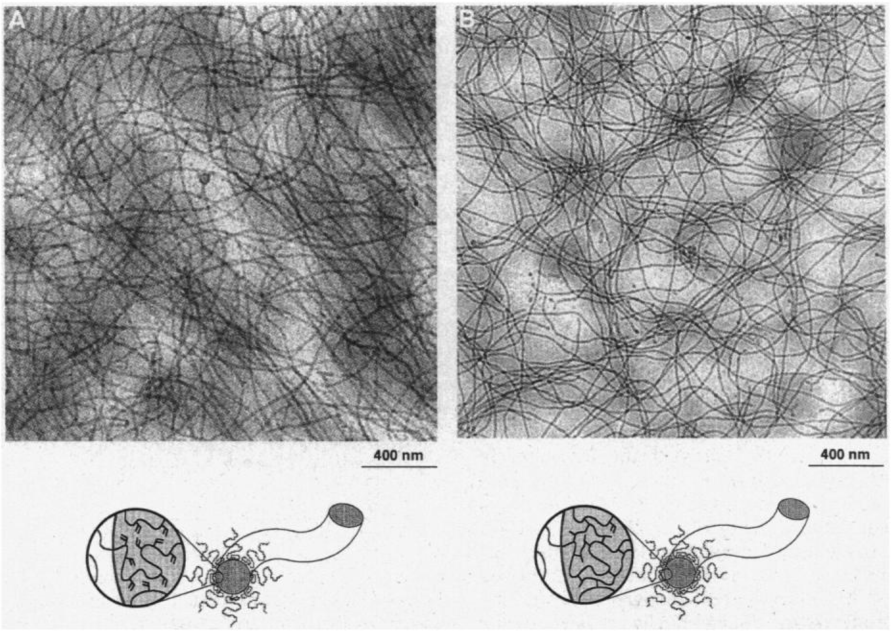

**Fig. 2.** Direct visualization of the 1% unreacted (**A**) and 0.05% cross-linked (**B**) wormlike micelles of **OB3** by CTEM. Sketches illustrate the local structure of pristine and cross-linked PB cores. Use of a lower concentration in (B) was necessitated by the gel-like character of the 1% cross-linked solution.

linked 3% solutions in heavy water ($D_2O$), plotted as intensity versus scattering wave vector $q = 4\pi\lambda^{-1} \sin \theta/2$ where $\theta$ and $\lambda$ are the scattering angle and radiation wavelength, respectively. By modeling these scattering results using established methodology (*9*) (solid curves), we have determined values for the core radius $R_c$ of 71 and 62 Å for the unreacted and cross-linked wormlike micelles, respectively (*10*). This reduction in $R_c$ with reaction exceeds that based on the densification that accompanies heavy cross-linking of rubber. The smearing in the scattering curves seen in Fig. 3A implies a distribution in core radii of $\Delta R_c/R_c \cong 11\%$ for both the pristine and cross-linked micelles.

SANS experiments also indicate that the cross-linking reaction is confined to the PB cores of the wormlike micelles. Solutions cross-linked at 5% block copolymer concentration could be diluted to arbitrarily low concentrations while remaining homogeneous. Figure 3B compares the low-$q$ scattering patterns obtained from two 0.5% solutions of cross-linked wormlike micelles. One was chemically fixed at a concentration of 0.5% and the other at 5% followed by dilution. These SANS patterns are virtually indistinguishable at all accessible $q$-values, which indicates that both solutions have the same intra- and intermicellar structure. Thus, our procedure appears to selectively transform the PB cores into cross-linked rubber without side reactions between micelles. By varying the concentration of redox initiator, the degree of core cross-linking can be precisely adjusted, thereby controlling the micelle stiffness and swelling characteristics.

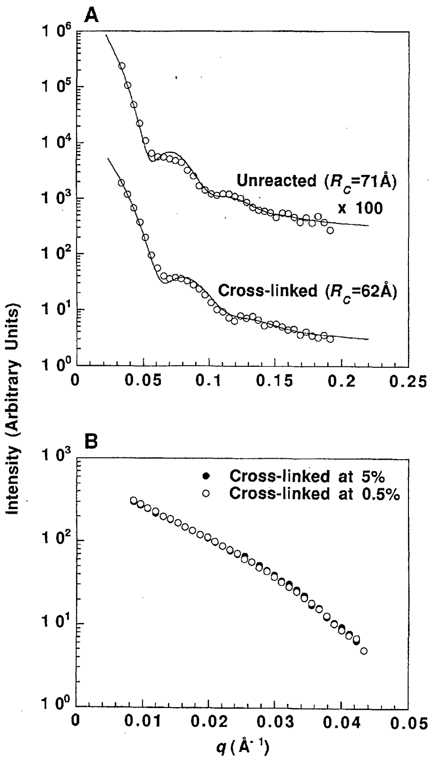

**Fig. 3.** SANS analyses of the wormlike micelles. (**A**) Three percent solutions of unreacted and cross-linked wormlike micelles. The solid curves represent the intraparticle scattering function for a system of long, stiff cylinders with core radius $R_c$, smeared for a radial polydispersity of $\Delta R_c/R_c = 0.11$. Data for the unreacted solution were shifted upward by a factor of 100 with respect to the cross-linked one. (**B**) Dispersibility of the cross-linked wormlike micelles is verified by a match between the intensity profiles of two 0.5% solutions of cross-linked wormlike micelles, one cross-linked at 5% and diluted and the other cross-linked at 0.5%.

The most striking effects of cross-linking are found in the viscoelastic properties of these giant wormlike micelles. Previous studies with wormlike micelles, especially those derived from cationic surfactants (*11*), have resulted in the concept of "living" micelles (*12*). When deformed, these threadlike objects behave like entangled macromolecules, except that they can pass through each other by breaking and re-forming, as first described theoretically by Cates (*12*). This mechanism produces a time-dependent shear modulus $G(t) = G_o e^{-t/\tau}$, where $G_o$ is a plateau modulus and $\tau = (\tau_{\text{break}}\ \tau_{\text{rep}})^{1/2}$, that is, the geometric mean between the characteristic micelle lifetime $\tau_{\text{break}}$ and the overall micelle reptation time $\tau_{\text{rep}}$. Our unreacted wormlike solutions display some similarity to conventional living micelle solutions (Fig. 4). However, cross-linking dramatically modifies this behavior. The dynamic elastic modulus $G'$ increased by more than two orders of magnitude and became solidlike (that is, frequency-independent) in the linear (small strain) regime. In the zero-shear limit, the 1% cross-linked solution appears to be a fragile gel (for example, entrained bubbles remain trapped indefinitely), whereas the living solution is clearly a liquid. A rise in the plateau level is not anticipated by the dynamic theory of Cates for flexible wormlike micelles (*12*) in the limit $\tau_{\text{break}} \to \infty$ (that is, no micelle breakage). This result suggests that cross-linking is accompanied by significant micelle stiffening, consistent with the transition from liquidlike to rubbery cores. These results represent the direct comparison of "living" versus "permanent" wormlike micelle properties.

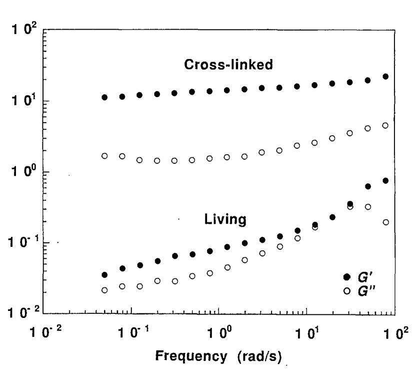

**Fig. 4.** Linear viscoelastic properties of 1% solutions of living and cross-linked wormlike micelles obtained by using a Couette geometry at room temperature; $G'$ and $G''$ represent the dynamic elastic and loss shear moduli, respectively.

Core cross-linking converts the "soft" block copolymer micelles, held together solely by van der Waals forces, into giant covalently bonded macromolecules. On the basis of measured core diameter and a rubber density of 0.90 g/cm$^3$, we estimate a molar mass of $\sim 2 \times 10^8$ g/mol per micrometer of micelle length. It is difficult to quantify the average micelle length from the CTEM images. Nevertheless, they are at least several micrometers long and possibly much longer. Thus, we have created wormlike molecules of molecular weight three or more orders of magnitude greater than large conventional synthetic polymers.

Experiments directed at cross-linking self-assembled systems composed of low molecular weight amphiphiles (lipids, surfactants, and soaps) (*13–15*) have met with limited success, and we are unaware of previous reports of chemical fixation of wormlike micelles. Cross-linking induces local perturbations that can overwhelm the delicate balance of forces that control particle size and shape. These effects are evidenced by the 13% reduction in core radius that accompanies cross-linking in **OB3**. However, by expanding the size of the micelle core through the use of polymeric amphiphiles, we have buffered the morphology against reaction-induced transformation. We expect this strategy to work with other morphologies including vesicles (*16*) and bicontinuous microemulsions (*17*, *18*).

### References and Notes

1. M. A. Hillmyer *et al.*, *Science* **271**, 976 (1996).
2. D. A. Hajduk, M. B. Kossuth, M. A. Hillmyer, F. S. Bates, *J. Phys. Chem. B* **102**, 4269 (1998).
3. M. A. Hillmyer and F. S. Bates, *Macromolecules* **29**, 6994 (1996).
4. T. M. Clausen *et al.*, *J. Phys. Chem.* **96**, 474 (1992).
5. Z. Lin, L. E. Scriven, H. T. Davis, *Langmuir* **8**, 2200 (1992).
6. Identification of the dark core region as PB was confirmed with higher magnification images where evidence of a PEO corona is visible.
7. G. Odian, *Principles of Polymerization* (Wiley, New York, ed. 3, 1991).
8. The actual bulk micelle concentration is not necessarily quantitatively reflected in the CTEM images because of differences in solution viscoelastic properties that result in thickness and concentration variations during specimen preparation.
9. J. S. Pedersen, S. U. Egelhaaf, P. Schurtenberger, *J. Phys. Chem.* **99**, 1299 (1995).
10. Wormlike micelles are characterized by complex SANS patterns that depend on specific contrast factors, micelle flexibility, and intermicelle corre-

lations. We have modeled the data appearing in Fig. 3A on the basis of a collection of noninteracting long, stiff cylinders, using just two levels of contrast. The associated core radii and polydispersities are relatively insensitive to these assumptions.
11. H. Rehage and H. Hoffmann, *Mol. Phys.* **74**, 933 (1991).
12. M. E. Cates, *Macromolecules* **20**, 2289 (1987).
13. H. Ringsdorf, B. Schlarb, J. Venzmer, *Angew. Chem. Int. Engl.* **27**, 113 (1988).
14. W. Srisiri *et al.*, *J. Am. Chem. Soc.* **119**, 4866 (1997).
15. W. Srisiri, A. Benedicto, D. F. O'Brien, *Langmuir* **14**, 1921 (1998).
16. D. D. Lasic, *Angew. Chem. Int. Ed. Engl.* **33**, 1685 (1994).
17. R. Strey, *Colloid Polym. Sci.* **272**, 1005 (1994).
18. F. S. Bates *et al.*, *Phys. Rev. Lett.* **79**, 849 (1997).
19. We thank D. Morse for valuable discussions. Supported by the Center for Interfacial Engineering (CIE) and the Materials Research Science and Engineering Center (MRSEC), both NSF-sponsored centers at the University of Minnesota. The SANS data were obtained at the Risø National Laboratory in Denmark with generous assistance from Kristoffer Almdal and Kell Mortensen.

10 November 1998; accepted 11 January 1999

# Ordered Mesoporous Polymers of Tunable Pore Size from Colloidal Silica Templates

**Stacy A. Johnson, Patricia J. Ollivier, Thomas E. Mallouk***

Ordered mesoporous polymers have been prepared by replication of colloidal crystals made from silica spheres 35 nanometers in diameter. The pores in the colloidal crystals were filled with divinylbenzene (DVB), ethyleneglycol dimethacrylate (EDMA), or a mixture of the two. Polymerization and subsequent dissolution of the silica template leaves a polycrystalline network of interconnected pores. When mixtures of DVB and EDMA are used, the pore size of the polymer replicas can be varied continuously between 35 and 15 nanometers because the polymer shrinks when the silica template is removed.

Template synthesis is a commonly used tool in the preparation of porous materials. Zeolites and related molecular sieves are commonly crystallized around small molecule templates, and mesoporous molecular sieves are templated by supramolecular aggregates of surfactant molecules (*1*) or by block copolymers (*2*, *3*). However, the size of the pores is limited to the dimensions of the organic templates (3 to 100 Å) and to materials such as oxides, chalcogenides, and phosphates that can be processed hydrothermally or solvothermally. Inorganic materials with much larger pores, in the size range of hundreds of nanometers to micrometers, have been synthesized with the use of vesicle arrays (*4*) or polymer spheres (*5*, *6*) as templates. Recently, colloidal crystals of silica spheres 150 to 300 nm in diameter have been used to make three-dimensional (3D) porous replicas composed of graphite, amorphous carbon, and diamond (*7*). Replication and embossing have also been used to make a wide variety of polymer structures with micrometer- and submicrometer-sized pores, most generally as thin films and freestanding membranes (*8*). In the case of embossed polymer thin films, the minimum feature size that can be faithfully replicated appears to be on the order of 10 nm (*9*).

The mesoscopic regime of 10 to 100 nm represents a largely unfilled gap for three-dimensionally ordered porous materials. Block copolymer templating has been used to access the lower end of this range with porous silicates. Arrays of hexagonal channels up to 30 nm in diameter and cubic structures with pore diameters in the 5- to 6-nm range have recently been prepared (*3*). Three-dimensional materials with pores in the 10- to 100-nm size range are of immediate interest for certain fundamental problems, such as the study of diffusion and phase equilibria in restricted geometries (*10*). They also have potential applications in the preparation of mesoscopic devices, such as ordered arrays of metal or semiconductor quantum particles (*11*) and in various sorption and separation processes involving polymers and biological macromolecules. Replica polymers, metals, and semiconductors have been prepared from one- and two-dimensionally porous template materials, including zeolites, mesoporous silicates, porous polymer membranes, anodic alumina, and clays (*12–20*). Imprint polymers that retain the shape and size of macromolecular templates have also been reported (*21*). These techniques usually produce individual particles of controllable shape and size, rather than 3D polymer networks with characteristic pore sizes and repeat distances between 10 and 50 nm.

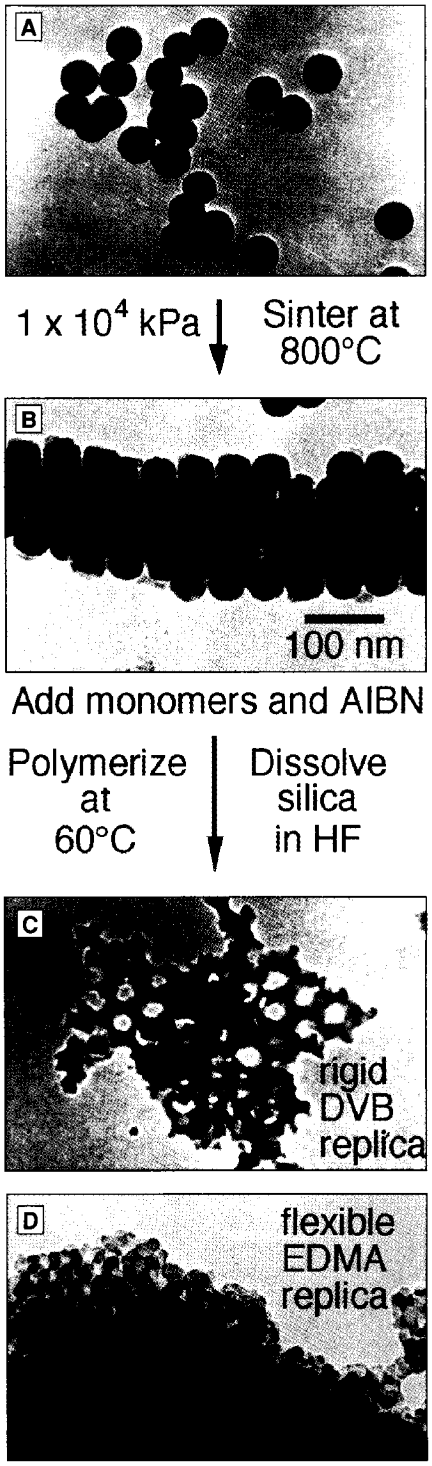

**Fig. 1.** TEM images of porous polymer preparation by replication. (**A**) Spherical silica particles as prepared. (**B**) Colloidal crystal of silica particles after pressing and heating. (**C**) DVB polymer replica. (**D**) EDMA polymer replica. The pore size in the flexible polymer is much smaller than the template diameter.

To create the inorganic template, monodisperse silica particles 35 nm in diameter were pressed into pellets at a pressure of 1 × $10^4$ kPa (*22*). The particles were sintered slightly at their points of contact by heating the pellets to 800°C, in order to provide pore connectivity in the polymer replica. Transmission electron mi-

---

Department of Chemistry, Pennsylvania State University, University Park, PA 16802, USA.

*To whom correspondence should be addressed. E-mail: tom@chem.psu.edu